Dynamics of Molecular Clouds: Observations, Simulations, and NIF Experiments

J. O. Kane, D. A. Martinez, M. W. Pound, R. F. Heeter, A. Casner, R. C. Mancini

January 23, 2015

Disclaimer

This document was prepared as an account of work sponsored by an agency of the United States government. Neither the United States government nor Lawrence Livermore National Security, LLC, nor any of their employees makes any warranty, expressed or implied, or assumes any legal liability or responsibility for the accuracy, completeness, or usefulness of any information, apparatus, product, or process disclosed, or represents that its use would not infringe privately owned rights. Reference herein to any specific commercial product, process, or service by trade name, trademark, manufacturer, or otherwise does not necessarily constitute or imply its endorsement, recommendation, or favoring by the United States government or Lawrence Livermore National Security, LLC. The views and opinions of authors expressed herein do not necessarily state or reflect those of the United States government or Lawrence Livermore National Security, LLC, and shall not be used for advertising or product endorsement purposes.

Dynamics of Molecular Clouds: Observations, Simulations, and NIF Experiments

Jave O. Kane *[a], David A. Martinez[a], Marc W. Pound[b], Robert F. Heeter[a], Alexis Casner[c], Roberto C. Mancini[d], [a]Lawrence Livermore National Laboratory, 7000 East Avenue, Livermore, CA, USA 94550; [b]Department of Astronomy, University of Maryland, College Park, MD 20742; [c]CEA/DAM/CESTA 15 Avenue des Sablières, 33114 Le Barp, France; [d]Department of Physics, University of Nevada, Reno, 1664 N. Virginia Street, Reno, NV 89503

ABSTRACT

For over fifteen years astronomers at the University of Maryland and theorists and experimentalists at LLNL have investigated the origin and dynamics of the famous Pillars of the Eagle Nebula, and similar parsec-scale structures at the boundaries of HII regions in molecular hydrogen clouds. Eagle Nebula was selected as one of the National Ignition Facility (NIF) Science programs, and has been awarded four NIF shots to study the cometary model of pillar formation. These experiments require a long-duration drive, 30 ns or longer, to drive deeply nonlinear ablative hydrodynamics. The NIF shots will feature a new long-duration x-ray source prototyped at the Omega EP laser, in which multiple hohlraums are driven with UV light in series for 10 ns each and reradiate the energy as an extended x-ray pulse. The new source will be used to illuminate a science package with directional radiation mimicking a cluster of stars. The scaled Omega EP shots tested whether a multi-hohlraum concept is viable — whether earlier time hohlraums would degrade later time hohlraums by preheat or by ejecting ablated plumes that would deflect the later beams. The Omega EP shots illuminated three 2.8 mm long by 1.4 mm diameter Cu hohlraums for 10 ns each with 4.3 kJ per hohlraum. At NIF each hohlraum will be 4 mm long by 3 mm in diameter and will be driven with 80 kJ per hohlraum.

Keywords: Eagle Nebula, NIF, laser, long duration, multi hohlraum, molecular clouds, cometary

1. INTRODUCTION

Figure 1. 1st panel: Eagle Nebula Pillars. Blue: O^{++}; green: H^+ red: S. 2nd panel: near infrared. 3rd panel: Pillars and illuminating star cluster in NGC3603. 4th panel: Geometry and orientation of the Pillars of the Eagle Nebula. Each Pillar also has some undetermined tilt angle into or out of the plane of the sky. The sizes of the star symbols show the relative luminosity of the irradiating stars, which are actually effectively point sources. Due to the "distance squared" falloff of a point source flux, the nearest and most luminous star provides most of the flux irradiating the Pillars. Adapted from Pound[27]. Image credits: Eagle: NASA/ESA/Hubble/Hubble Heritage Team (2015). NCG3603: HST + VLT/ISAAC[5] (2000).

A laboratory astrophysics experiment is being fielded at the National Ignition Facility (NIF) to determine velocity and density profiles in star-forming HII pillars of molecular clouds such as the Eagle Nebula (**Figure 1**). In companion efforts, models for the measured profiles are being vetted and the utility of new observations of these structures assessed. NIF is a large, 192-beam 2 MJ laser at Lawrence Livermore National Laboratory used for fusion research, national security studies, and basic science. The university-led NIF Science committee selected the Eagle collaboration as one of

nine science programs eligible to apply for NIF user shots. NIF is the first HED facility that can generate a radiation source sufficiently collimated, intense, and long lasting to drive cometary flows and directional instabilities in scaled laboratory experiments, and permit assessment of models for producing flows generating pillars. In a Department of Energy/NASA effort spanning 16 years, theorists, astronomers and experimentalists have assessed models for the origin and evolution of pillars using radiative hydrodynamics simulations, millimeter-wave observations of the Eagle and Horsehead nebulae at the Berkeley-Illinois-Maryland Association (BIMA) and Combined Array for Research in Millimeter-wave Astronomy (CARMA) radio telescope arrays, and recently, laser experiments to develop an illuminating source that mimics a cluster of stars. Major results of our work are that the Rayleigh-Taylor instability is strongly suppressed by ablative stabilization in the context of HII regions, while a cometary model may explain pillar-like structures.

As a step towards quantitatively assessing these conclusions, NIF is being used to generate cometary structures and to determine the velocity and density profiles of the tails. NIF is used to illuminate scaled, clumpy low-density targets representing molecular clouds, using a laser-generated x-ray source representing a cluster of O-type stars. To generate deeply nonlinear, hydrodynamic evolution with significant shadowing of the illumination by clumps, a new high power, long duration, directional source has been developed that uses multiple radiation cavities (hohlraums). In June 2013 a smaller-scale prototype of the experiment was tested at the 16 kJ Omega EP laser at the University of Rochester Laboratory for Laser Energetics (LLE), validating the performance of the source using shock and spectroscopic measurements. These shots also demonstrated a science package relevant to photoionized fronts and accretion disks[19, 20]. In March 2014 further Omega shots, a smaller version of a target serving as a scaled version of a clumpy molecular cloud was deployed, and techniques were developed to image cometary structure.

With these results in hand[4], NIF shots are being performed using larger-scale targets and 20 times the energy used at Omega EP. Omega EP delivers enough energy to drive a shock past a clump, while NIF can ablate enough material to form a cometary tail confined by ablative pressure behind the clump. The long NIF drive can also allow access to new dynamics unique to long-duration, directed illumination.

2. BACKGROUND

Molecular clouds are the birthplaces of stars. Comprised principally of molecular hydrogen with trace amounts of dust (10^{-2} by mass), carbon monoxide (10^{-4} by volume) and other species, molecular clouds have typical masses of 10^4 -10^6 solar masses, sizes of tenths to tens of parsecs, average molecular hydrogen number density of 10^3 cm^{-3}, and average bulk temperatures of about 10 K[38]. The most massive O and B stars born in a molecular cloud are hot, with photospheres at temperature of a few tens of thousands of K[6], and give off high-intensity UV photons. These UV photons irradiate the parent molecular cloud and photoevaporation occurs, resulting in a stratified structure. The photoevaporative (ablated) flow is normal to the molecular surface[10]. The region between the OB stars and the molecular cloud surface is the H II region, in which the hydrogen gas is almost fully ionized, and photoionization and recombination to neutral atomic hydrogen occurs in steady state. The ionization front (IF) is a very thin layer because of the short mean free path for the incident photons on the cloud surface. At the surface all the photons above the Lyman limit are absorbed.

Photons below the ionization limit but above 11.2 eV cannot ionize the hydrogen atom in the ground state but can penetrate the IF and dissociate the molecular hydrogen in the underlying layers. The thickness of the dissociation front differs with each cloud, but is typically of order 10^{16} cm. The last layer in the stratified structure is the molecular gas. Because of strong radiative cooling, the molecular cloud temperature is typically a few tens of K[26]. The dynamics of irradiated molecular clouds are thought to play a role in star formation[2, 42, 18]. Consequently, the outflow dynamics from the molecular cloud into the H II regions are of considerable, general interest[27,21].

Although molecular hydrogen (H_2) is the dominant molecular species in clouds and governs their dynamical and chemical evolution, its lacks a dipole moment and can only change rotational-vibrational state through weak quadrupolar transitions that are only rarely detectable. Alternative means of determining the physical conditions of molecular clouds have therefore been developed over the years; many use of a tracer species (a molecule or dust) that is easier to detect, and infer the molecular hydrogen content by some proportionality relation. One of the most commonly used tracers of molecular gas is carbon monoxide (CO), which is collisionally excited by H_2. CO readily emits under the conditions typically found in molecular clouds and is easily observed at millimeter wavelengths with ground-based facilities.

The shapes of the surfaces between molecular clouds and the H II regions around massive stars typically feature elongated structures, commonly referred to as pillars, columns, spikes, or elephant trunks[10, 27, 28, 2]. The surface is a photoionization front driven by the strong UV radiation from the OB stars. Perhaps the most spectacular – and certainly most studied – example is the Eagle Nebula, which has three large, molecular pillars near a small group of O stars[11] (**Figure 1**).

Distance	1900 pc	Total mass	800 solar masses
Characteristic length scale	1 pc	Thermal pressure (P/k)	10^6 K cm^{-3}
Interior temperature	40 K	Turbulent pressure (P/k)	10^8 K cm^{-3}
Bulk velocity	25 km/s	Column density	10^{22} cm^{-2}
Velocity gradient in molecular gas	~10 km/s/pc	Dynamic timescale	105 years
Velocity dispersion in molecular gas	1 km/s	Evaporative timescale	10^7 years
Velocity of ablation flow	20 km/s	Plane of sky rotation, θ	39 degrees
Peak H_2 number density	10^5 cm^{-3}	Line of sight inclination, i	~10 degrees
H ion number density in ablation flow	10^3 cm^{-3}	Magnetic field	not yet measured

Table 1. Observational Summary of the Eagle Nebula Pillars

2.1 Observations of Pillar structures

In the time since the Hubble Space Telescope image[10] made headlines around the world, there have been several studies of the Eagle Pillars and their environs, from radio to infrared to optical to x-ray wavelengths[27, 44, 16, 42, 12, 17]. Thus the observational picture of the Eagle Pillars is fairly complete and the measurements can give solid constraints on any formation model (Table 1). The Eagle Nebula is 1900 pc (5700 light years) from the Solar system[11]. It is estimated that half of the ionizing radiation comes from a single O3–4 star and the rest mostly comes from three other nearby stars with spectral types O5–O6[10]. The total ionizing flux from the stars is estimated to be S = 1-2 x 10^{50} s^{-1}. The temperature in the H II region near the molecular cloud surface is 9500 K, and the ionized hydrogen number density is 5000 cm^{-3} 16. The photodissociation region (PDR) is relatively thin because the large hydrogen number density n(H2) ~ 1000 cm^{-3} provides high optical depth.

Radio wavelength observations have provided much information about the dynamics of the gas in the pillars. As measured by CO line observations the velocity gradients along the long axes of the pillars (from 'head' to 'tail') are between -20.7 and +6.7 km/s/pc, with an average magnitude of 8.3 km/s/pc. Furthermore, the pillars are not in the same plane in the sky; the differing signs of the velocity gradients indicate inclination toward (positive gradient) or away (negative gradient) from the observer. Predictions of the simple classical Rayleigh-Taylor (RT) instability theory with regard to the velocity gradient[8], are incompatible with the observed gradient, at least for constant acceleration[27]. Recently millimeter-wave observations of the Pelican Nebula were performed at CARMA, partly to help assess choices of targets for the NIF Eagle experiments.

2.2 Mechanism for the formation of Pillar structures

Although a number of observational, theoretical and numerical studies have been carried out, the formation mechanism of pillars beside massive stars is still not fully understood. The discussion falls into two classes. In one class, pillars are formed due to dense, preexisting cores in the molecular cloud that shield material behind them from ionizing and dissociative processes[30, 4, 15, 45]. This is commonly referred to as the cometary model because the resulting dense head and long tail superficially resemble a comet. Another possibility is that the pillars are caused by hydrodynamic instabilities. Spitzer[39] suggested that the pillars in the Eagle Nebula result from the nonlinear stage of the Rayleigh Taylor (RT) instability occurring at the contact discontinuity between the dense molecular cloud and the lower density, hot photoevaporated plasma. Frieman[8] estimated the timescale of the instability to be less than 10^6 yr. Vandervoort[43] found another type of instability at the IF in a non-accelerating frame, the so-called IF instability, which, in his analysis, was present in the case of non-normal incident radiation. He derived a dispersion relation for perturbations growing by this process. Axford[1] extended it to include recombination, which plays a crucial role in the H II region. Recombination

in the ionized gas works to smooth the surface when the wavelength of the perturbation is larger than the recombination length.

2.3 Previous Relevant work by this Collaboration

Over the past 16 years, our group has made significant progress towards understanding the behavior of photoevaporated clouds and linking this understanding to the astrophysical observations. We have developed a comprehensive 2-D hydrodynamic model of pillar formation that includes: energy deposition and release due to the absorption of UV radiation; recombination of hydrogen; radiative molecular cooling; magnetic pressure; and geometry/initial conditions based on Eagle observations. In the process, we have developed a theory for magnetostatic support in molecular clouds as well as a model for photoevaporation front instability which accounts for acceleration of the front, temporal variation of the ionizing radiation intensity, tilt of the radiation flux with respect to the surface normal, and partial absorption of incident radiation in the ablated material. We have examined pillar formation due to both ionization-front instability and shadowing by dense cores. To facilitate comparison between models and astronomical observations, we have also prototyped a process to create 'synthetic observations' from the model.

Basic Scalability

The spatial and temporal scales of astrophysical phenomena are typically 10–20 orders of magnitude greater than those of laboratory experiments intended to simulate them. Accordingly, the issue of similarity between the astrophysical phenomenon and its laboratory counterpart becomes quite important. In astrophysics, one is often dealing with highly dynamical systems, where orders of magnitude variation of the parameters of interest occurs over the duration of an event. We have studied astrophysical phenomena that can be reasonably well described by magnetohydrodynamic (MHD) equations and formulated a broad class of similarities that can be applied to them, including situations where the transition to turbulent flows occurs. A broad variety of astrophysical objects and configurations can be adequately simulated in high-energy-density laboratory experiments. In particular, we have theoretically examined the possibility of scalable experiments directed towards studies of photoevaporated molecular clouds.

Of interest here are the nonlinear dynamics of radiatively driven, cold, tenuous molecular clouds. Remarkably, the hydrodynamic description is valid. Also remarkably, this same hydrodynamic description works in the laboratory experiments, where the spatial and temporal scales are, roughly speaking, 20 orders of magnitude smaller. (There area also numerous astrophysical processes that cannot be adequately described by hydrodynamics.) Designing a scalable experiment involves ensuring that the same set of equations adequately describe both the astrophysical and laboratory scenario, choosing initial conditions satisfying similarity requirements, and determining time interval within which boundary effects and possible development of small scales will not significantly affect the laboratory model. There are already several examples (related mostly to the simulation of the supernova hydrodynamics) where all these steps have been taken and allowed producing substantial scientific information[32]. The broad applicability of ideal gas hydrodynamics in astrophysics is related in part to the very large geometrical scales of astrophysical systems. This makes the smallness of the particle mean-free path compared to the global length-scale a rather common occurrence. However, hydrodynamics of an ionized medium may work well even beyond these conditions of direct applicability. An example is a tangled magnetic field: even if it is very weak, it may imitate real collisions in a number of situations[32, 7]. The cold interior of molecular clouds like the Eagle Nebula present an additional challenges: the ionization degree is small, and sub-micron carbon-containing dust grains constituting $\sim 10^{-2}$ of the cloud mass generate non-thermal ionization due to cosmic rays to which the clouds are transparent. A substantial fraction of the electrons are probably attached to the dust grains. Estimates of the fraction of dust grains that are ionized, x_i, for the conditions typical for the Eagle Nebula yield $x_i < 3\times10^{-8}$. This yields a lower-bound estimate of the electrical conductivity, which ought to be relatively high. An estimated magnetic diffusion time is then $\sim 10^{13}$ years, comfortably long to make a non-resistive MHD a good approximation (note that the age of the Eagle nebula pillars is $\sim 10^{5}$ years). Viscosity and thermal conductivity in the medium are negligible, because of very large spatial scales involved. So, we conclude that ideal MHD is a reasonable description of weakly ionized gas in the Eagle Nebula.

Magnetic Stiffness

Within the larger context of how pillars form, there are detailed physics questions about our understanding of molecular cloud dynamics. One such question concerns how do the clouds maintain pressure balance against the pressure from the

ablative flow. The thermal pressure is 10-100 times too low; and large velocity line widths measured in CO are evidence that some form of non-thermal pressure is present (see, *e.g.* Table **1**). Supersonic turbulence will decay in a crossing time of the driving scale and both hydrodynamic and MHD turbulence decay in less than a free-fall time[9, 40]. A new mechanism of 'magnetostatic turbulence' has been proposed as a possible explanation. Our group has examined the potential role of this lasting nearly force-free turbulence as a source of cloud 'stiffness' such that the cloud behaves as a polytropic gas with adiabatic index of $\gamma = 4/3$ [35, 36, 37]. This opens the possibility of simulating the Eagle Nebula in a traditional setting, without any need to impose a very strong magnetic field. Magnetostatic turbulence provides sufficient stiffness even if the gas is cold, close to its initial temperature ~0.003 eV (to which gas cools down at a very short distance behind the initial shock). Tangled magnetic fields could be generated by shear flows and shear turbulence in the initial cloud. Pre-existing magnetic field could be relatively weak but the compression of the cloud under the action of the ablation pressure would increase it to the values required to provide sufficient stiffness.

Radiative Hydrodynamic Simulations of the Eagle Nebula

Our group has performed extensive hydrodynamic simulations of the Eagle Nebula to identify mechanisms for Pillar growth and compare predictions to astronomical observations. Free streaming transport of incident photons, simplified radiative processes, and ideal gas equations of state (EOS) are used. The radiative processes considered are absorption of incident photons, radiative cooling via recombination of ionized hydrogen, and radiative cooling in the molecular cloud. We make the simplifying assumption that reradiated photons escaped the cloud (i.e., are not redeposited or transported). We also include an ad hoc magnetic stiffness term in the EOS, motivated by observations of the Eagle Nebula, and our theoretical studies[33].

Simulations in planar geometry immediately suggested that ablative stabilization due to 'plasma filling' strongly damps RT growth of modest initial perturbations, as follows[22, 23]. Any small concavity at the photoevaporation (ablation) front causes slight focusing of the ablated plasma, increasing density in the converging ablation flow and enhancing recombination, greatly increasing the optical depth to incoming UV drive photons. Nearby protuberances in the surrounding ridge of the perturbation are still strongly irradiated and driven. Hence, the concavity is smoothed out. For a very large initial 'perturbation' amplitude, the ionization front strongly separates from the ablation front, and ablation pressure drops significantly at the vertex of the concavity, causing it to invert into a spike[24] that then grows by cometary flow due to shadowing of the steep walls.

In contrast, our modeling in cylindrical 2D geometry (**Figure 2**) show that cometary flow can reproduce observations of density and velocity in the Eagle Nebula. The spherical initial cloud has a power law density profile in the outer cloud and a central core of constant density. The dense core prevents the developing pillar from translating a considerable distance from the illuminating source. (In Lefloch[15], the initial clouds were of constant density, and the final structure had moved five to ten times its final length.) The star is initially 2 pc from the core. In these simulations the model of turbulent magnetic support pressure is generalized to be spatially varying to avoid extremely high fields in the initial core. The energy deposition is significantly advanced as in Richling[31] and Yorke[46]: UV rays are traced obliquely versus being simply attenuated down columns. The steep sides of the cometary pillar in **Figure 2** result when ablated plasma is confined behind the initial core clump due to shadowing of the sustained, directional radiation. In the proposed NIF shots, scaled targets with graded-density targets will mock up initial conditions like those used in these astrophysical simulations.

Developmental shots at Omega EP laser

In 2013 and 2014 our group tested a smaller-scale prototype of the proposed NIF experiment at the Omega EP laser at the University of Rochester Laboratory for Laser Energetics (**Figure 3** and **Figure 4**). Shots in June 2013 (**Figure 3**) validated the performance of the x-ray source using shock and spectroscopic measurements. These shots also demonstrated a photoionization science package. In March 2014 shots (**Figure 4**) a second science package, the Eagle science package, was deployed. The package was a small-scale version of a clumpy molecular cloud target. Techniques to image early-stage cometary structure were also tested. **Figure 3** shows the long-duration radiator source used in the June 2013 shots[14]. The source was simply a few-mm wide Cu block drilled through in four places to create a multi-tube radiator. Three of the tubes (hohlraums) were used. The tubes were illuminated one after another by the laser, each tueb

receiving 4 kJ of laser energy over 10 ns, for total pulse energy of 12 kJ and pulse length of 30 ns. Each tube contained a novel air-density foam fill developed for this experiment to mitigate laser reflection. The laser-heated foam fill and the copper walls reradiated in x-rays, which were used to illuminate the science package.
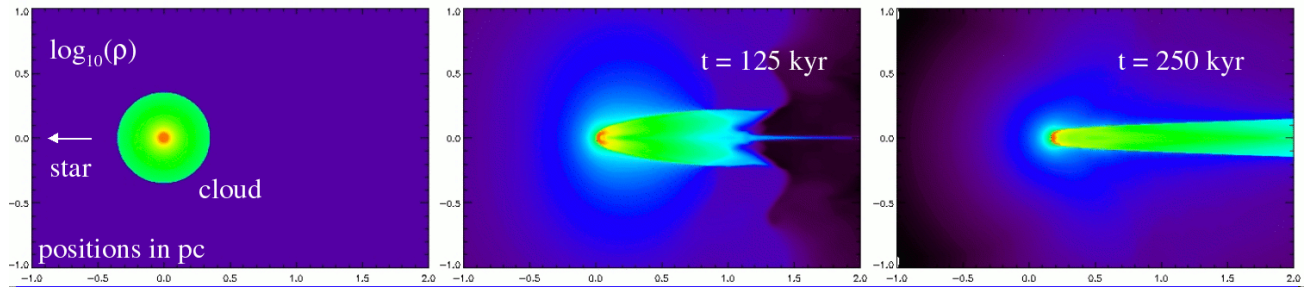

Figure 2. Log density contours at three time steps in a 2D cylindrical radiation hydrodynamics simulation of a cometary pillar. A 30 solar mass cloud initially 2 parsecs (6 light years) from an O-type UV star undergoes ablation and photoevaporation, and accelerates by the rocket effect. A cometary tail is confined behind the clump by its own ablative pressure. The initial cloud has a very dense core and a power law density gradient outside the core. Eagle Pillar 2 is believed to be about 125 kyr old as in the middle panel.
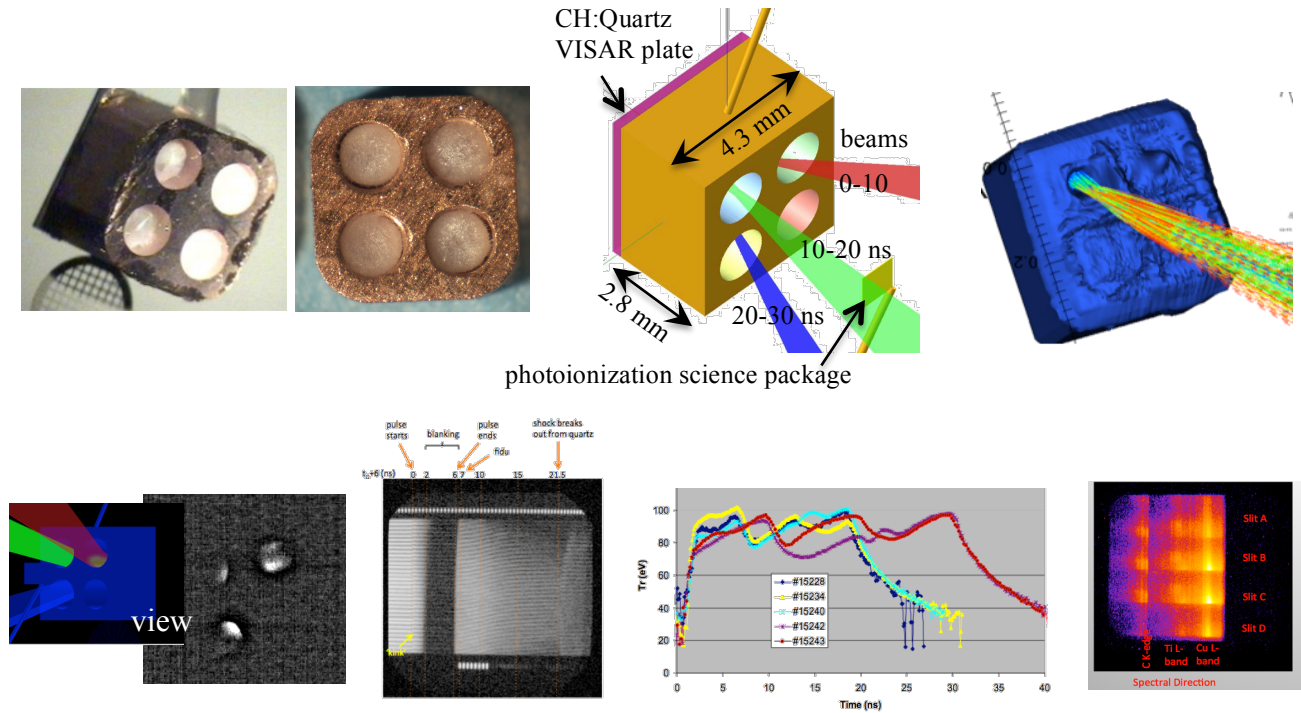

Figure 3. 2013 Omega EP experiments. Top: 1st panel: the source was a Cu block with four drilled hohlraum tubes, to mock up a cluster of stars. 2nd panel: 4 mg/cc CH foam fill was used to delay tube closure and mitigate glint. 3rd panel: three of four tubes were illuminated by EP laser beams, one after another for 10 ns each, generating a 30 ns drive of x-rays radiated from the foam fill and the inner walls of Cu tubes. A VISAR package was mounted on the back end of the source to measure the strength of a shock driven into the package by the x-rays and verify the source performance. A first science package, a Ti photoionization sample, was mounted 4 mm from the other end of the tubes. 4th panel: 50% critical surface in 3D HYDRA radiative hydrodynamics simulation with a laser source predicts that even for the fourth tube, the EP beam could enter the tube without being absorbed or deflected by plumes from the tubes driven earlier. Bottom: 1st panel: late-time pinhole x-ray images of the source during the shots shows tubes lighting up, with earlier tubes having cooled. 2nd panel: the ASBO record shows a strong shock propagating through through the CH:quartz VISAR package in good agreement with HYDRA simulations. 3rd panel: pulse lengths of 6 ns and 10 ns (per tube) were tested; the DANTE x-

ray flux measurements show good reproducibility between shots and showed that the third tube radiated as strongly as the first. 4th panel: Ti spectra were obtained from the photoionization science package.
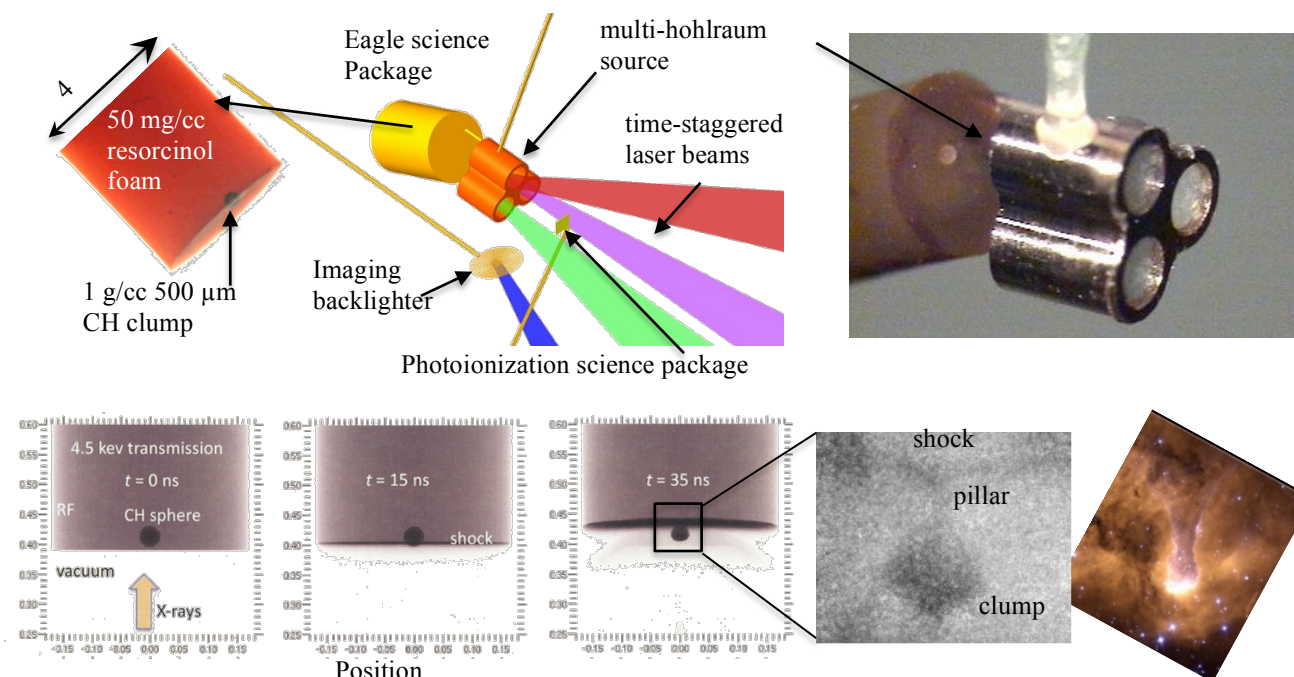

Figure 4. Omega EP 2014 shots. Top: A refined three-tube, 30 ns source is used. The VISAR package is removed, opening the back end of the tubes. A preliminary Eagle science package, a 1g/cc CH clump embedded in 50 mg/cc foam, is stood off 2 mm from the source to see directional illumination. Bottom left three panels: simulated x-ray radiographs of an evolving early-stage pillar in a HYDRA simulation of the experiment. A shock is driven just past the clump. Bottom 4th panel: the clump actually shot was 35% smaller than designed, allowing the shock to move well past the clump, and a narrow tail of shocked background material to collect behind the clump. Bottom 5th panel: visible light image of NGC 3603 for comparison.
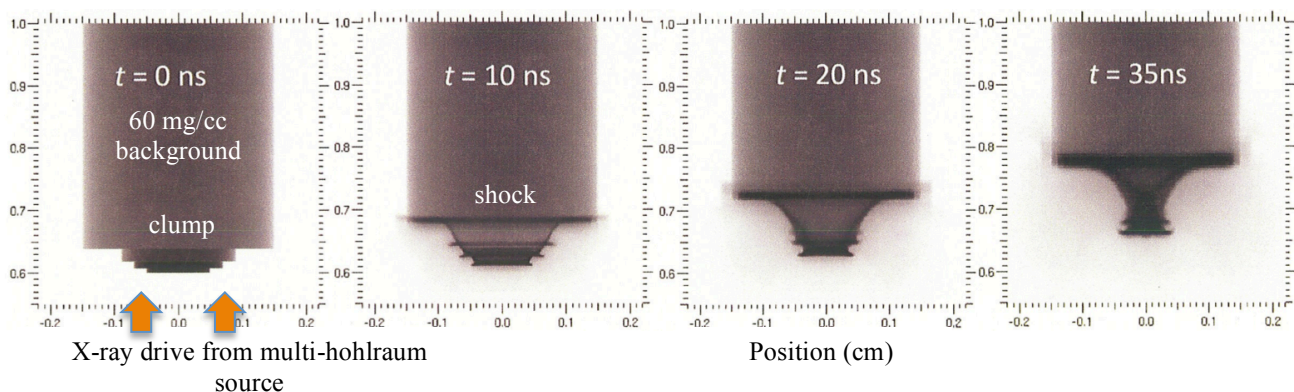

Figure 5. Simulated x-ray radiographs of an evolving pillar in a HYDRA model of the planned Eagle NIF experiment: With 240 kJ (20 x the energy used in the Omega EP experiments) and a graded-density clump in an science package placed 5 mm from the source, a cometary tail is confined behind the clump by its own ablative pressure. The tail is composed of background material shadowed by the clump, as well as material removed from the clump by ablation and shock acceleration.

In a set shots performed in March 2014 (**Figure 4**), the VISAR package was removed and an Eagle physics package consisting of a CH clump embedded in a background low-density resorcinol foam was stood off a few mm from the back end of the source so that the package saw illumination only from the direction towards the ends of the tubes. The mass of

the source itself was reduced to mitigate debris formation. The μDMX spectrometer data (not shown) demonstrated that the source generated a 90 EV x-ray output. A key task in these shots was to develop an x-ray backlighting scheme that could be used at NIF to image the pillar structure in transmission. **Figure 4** shows a backlit image from one of the shots. In the image, taken at 35 ns, after the third laser beam has shut off, the shocked CH clump is visible, as is the shock propagating into the foam. This preliminary imaging technique will be refined at NIF, with a larger image region, much more energy available for the backlighter, and tuned backlighter and filtering materials. As shown in **Figure 4**, the backlit image obtained corresponds well to predictions of the radiative hydrodynamics code HYDRA .
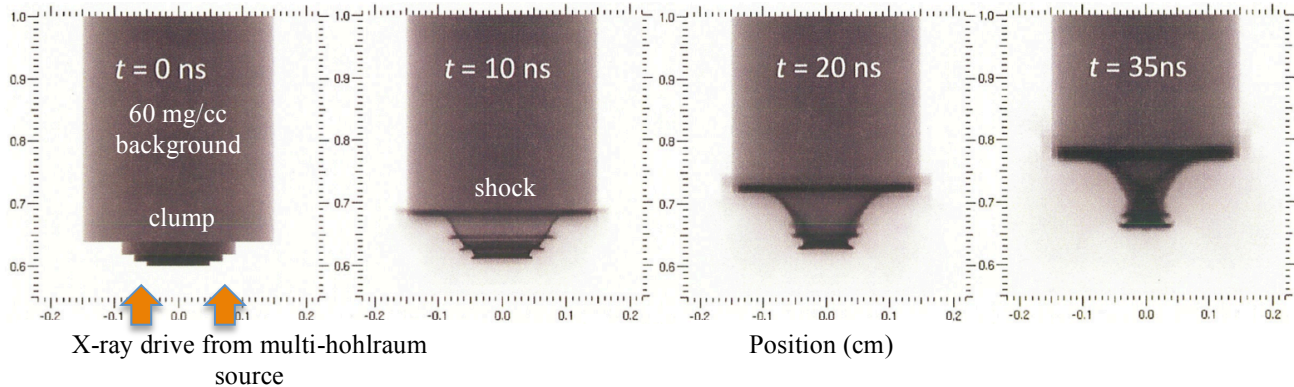

Figure 5 shows simulated radiographs from a 2D HYDRA model of the planned NIF experiment. The NIF Eagle science package consists of a background foam of 60 mg/cc carbonized resorcinol foam (CRF), with a clump placed on the surface of the background foam. The clump is composed of three layers of CH plastic and CRF of decreasing density and increasing diameter, with the densest layer facing the drive. For the NIF shots, a three-tube source is used, similar to the one used at Omega EP (**Figure 4**) but larger, 2.7 mm in diameter by 3.5 mm in length. Each tube is illuminated for 10 ns with 80 kJ of laser energy, for a total laser of energy of 240 kJ, 20 times the amount of energy used in the Omega EP experiments. With the increased energy at NIF, the x-ray drive from the source is able to push a shock well past the clump, forming a distinct pillar composed of background foam pushed in behind the clump, as well as material released from the clump by the propagating shocks and by ablation. The heavy clump moves only a few hundred μm during the experiment while the ablating shocked surface of the background moves on the order of a millimeter.

The goals in the initial NIF experiments are to confirm the performance of a long-duration, multi-hohlraum source at NIF scales and energies; to robustly generate a pillar to test the x-ray diagraph diagnostics; and to validate the HYDRA radiative hydro modeling. The validate HYDRA model can then be used to determine the velocity and density profiles in the pillar and permit comparisons to density and velocity profiles observed in the Eagle and other astrophysical pillars. In more advanced experiments, it may be possible to generate and diagnose lower density pillars; assessments of possible diagnostics for such experiments will be carried out at the Omega EP laser.

REFERENCES

[1] Axford 1964] W.I. Axford, "The stability of ionization fronts," Ap.J. 140, 112 (1964).
[2] [Bally 2003] J. Bally and B. Reipurth, "Irradiated jets and outflows in the Pelican Nebula," AJ 126, 893 (2003).
[3] [Berne 2010] O. Berne, N. Marcelino, and J. Cernicharo, Nature, 466, 947 (2010).
[4] [Bertoldi 1990] F. Bertoldi and C. F. McKee, Astrophys. J. 354, 529-548 (1990).
[5] Brandner, E. Grebel ,Y. H. Chu, et al Astron.. J 119, 301 (2000).
[6] [Dors 2003] Dors, O.L, Copetti, M.V.F., A&A, 404, 969 (2003).
[7] [Drake 2000] Drake R P, Phys. Plasmas 7, 4690 (2000).
[8] [Frieman 1954] E.A. Frieman, "On 'elephant-trunk' structures in the region of O associations," Ap.J. 120, 18 (1954).
[9] [Goldreich 1974] P. Goldreich and J. Kwan, "Molecular clouds," Ap.J. 189, 441 (1974).
[10] [Hester 1996] J. Jeff Hester, et al., Astron. J. 111, 2349 (1996).
[11] [Hillenbrand 1993] L.A. Hillenbrand, et al., "NGC-6611: a cluster caught in the act," AJ 106, 1906 (1993).
[12] [Indebetouw 2007] R. Indebetouw et al., Ap.J. 666, 321 (2007).

[13] [Kane 2005] J.O. Kane, D.D. Ryutov, A. Mizuta, B.A. Remington, and M.W. Pound, "Molecular clouds: observation to experiment," Astrophys. Space Science Vol. 298, No. 1-2, 261-265 (June, 2005).

[14] [Kane 2013] J.O. Kane et al., "Preliminary Report on HEDLP/LBS Long-Duration Radiation Sources Experiment on Omega-EP", LLNL-TR-639652, June 21 (2013).

[15] [Lefloch 1994] B. Lefloch and B. Lazareff, AA 289, 559 (1994).

[16] [Levenson 2000] N. Levenson, et al., Astrophys. J. Lett. 533, L53-L56 (2000).

[17] [Linsky 2007] Jeffrey L. Linsky et al, Ap.J. 654, 347 (2007).

[18] [McCaughrean 2002] McCaughrean, M.J., Andersen , M., A&A, 389, 513 (2002)

[19] [Mancini 2009] "Accretion disk dynamics, photoionized plasmas, and stellar opacities" R. C. Mancini, J. E. Bailey, J. F. Hawley, T. Kallman, M. Witthoeft, S. J. Rose and H. Takabe, Physics of Plasmas 16, 041001 (2009).

[20] [Mancini 2011] "Radiation hydrodynamic simulation of a photoionized plasma experiment at the Z facility" I. M. Hall, T. Durmaz, R. C. Mancini, J. E. Bailey and G. Rochau, Astrophysics and Space Science 336,189 (2011).

[21] [Mizuta 2002] Akira Mizuta, Shoichi Yamada, Hideaki Takabe, ApJ, 567, 635 (2002)

[22] [Mizuta 2005a] Akira Mizuta, Jave O. Kane, Marc W. Pound, Bruce A. Remington, Dmitri D. Rytov, and Hideaki Takabe, "Hydrodynamic instability of ionization fronts in H-II regions," Ap. J. 621, 803 (March 10, 2005).

[23] [Mizuta 2005b] Akira Mizuta, Hideaki Takabe, Jave O. Kane, Bruce A. Remington, Dmitri D. Ryutov, and Marc W. Pound, Astrophys. Space Science Vol. 298, No. 1-2, 197-202 (June 2005).

[24] [Mizuta 2006] Akira Mizuta, Jave O. Kane, Marc W. Pound, Bruce A. Remington, Dmitri D. Ryutov, and Hideaki Takabe, "Formation of Pillars at the Boundaries between HII Regions and Molecular Clouds," Ap.J. 647, 1151 (2006).

[25] [Mizuta 2007] Akira Mizuta , Jave O. Kane, Marc W. Pound , Bruce A. Remington, Dmitri D. Ryutov, and Hideaki Takabe, "Nonlinear Dynamics of Ionization Fronts in HII Regions," Ap.S.S. 307, 183 (Jan., 2007).

[26] [Neufeld 1995] Neufeld, A.A., Lepp, S., Melnick, G.J., ApJS, 100, 132 (1995)

[27] [Pound 1998] Pound, M.W., "Molecular Gas in the Eagle Nebula," Ap.J.Lett. 493, L113 (1998).

[28] [Pound 2003] Pound, M.W., Reipurth, B., Bally, J., "Looking into the Horsehead," AJ, 125, 2108-2122 (2003).

[29] [Pound 2007a] Pound, M.W., Kane, J.O., Ryutov, D., Remington, B.A., Mizuta, A., AP&SS, 307, 187-190 (2007).

[30] [Reipurth 1983] B. Reipurth, Astron. Astrophys. 117, 183 (1983).

[31] [Richling 2000] Richling S., and Yorke, H.W. 2000, ApJ, 539, 258 (2000)

[32] [Ryutov 2001] D.D. Ryutov, B.A. Remington, H.F. Robey, and R.P. Drake, Phys. Plasmas 8, 1804 (2001).

[33] [Ryutov 2002] D.D. Ryutov and B.A. Remington, "Scaling astrophysical phenomena to high-energy-density laboratory experiments," Plasma Phys. Control. Fusion 44, B407 (2002).

[34] [Ryutov 2003] D.D. Ryutov, J.O. Kane, M.W. Pound, B.A. Remington, "Instability of an ablatively-accelerated slab in the case of non-normal irradiation," Plasma Phys. Contrl. Fusioon 45, 769 (2003).

[35] [Ryutov 2005a] D.D. Ryutov, J.O. Kane, A. Mizuta, M.W. Pound, B.A. Remington, "Two models of magnetic support for photoevaporated molecular clouds," Astrophys. Space Science Vol. 298, No. 1-2, 183-190 (June 2005).

[36] [Ryutov 2005b] Ryutov, D., Kane, J.O., Mizuta, A., Pound, M.W., Remington, B.A., Two Models of Magnetic Support for Photoevaporated Molecular Clouds, Ap&SS, 298, 183-190 (2005).

[37] [Ryutov 2007] D.D. Ryutov, J.O. Kane, A. Mizuta, M.W. Pound, and B.A. Remington, "Phenomenological theory of the photoevaporation front instability," Ap.S.S. 307, 173 (Jan., 2007).

[38] [Shu 1987] Shu, F., Adams, F., Lizano, S., ARA&A, 25, 23 (1987)

[39] [Spitzer, 1954] Lyman Spitzer, Jr., "Behavior of matter in space," Ap.J. 120, 1 (1954).

[40] [Stone 1998] J.M. Stone, E.C. Ostriker, C.F. Gammie, Ap. J. 508, L99 (1998).

[41] [Stone 2008] The Astrophysical Journal Supplement Series 178, 137 (2008).

[42] [Sugitani 2002] K.Sugitani, et al., Astrophys. J. Lett. 565, L25-L28 (2002).

[43] [Vandervoort 1962] P.O. Vandervoort, "Stability of ionization fronts," Ap.J. 135, 212 (1962).

[44] [White 1999] G.J. White, et al., Astron. Astrophys. 342, 233 (1999).

[45] [Williams 2001] R.J.R. Williams, D. Ward-Thompson, and A. P. Whitworth, "Hydrodynamics of photoionized columns in the Eagle Nebula, M16," Mon. Not. R. Astron. Soc. 327, 788-798 (2001).

[46] [Yorke 1995] Yorke, H., and Kaisig, M., Comp. Physics. Comm, 89, 29 (1995)